

Components of the Shape Revisited

Sibel Tari

Middle East Technical University
Ankara, TR-06531
stari@metu.edu.tr

Bernhard Burgeth

Saarland University
Saarbruecken, DE-66041
burgeth@math.uni-sb.de

Ilker Tari

Middle East Technical University
Ankara, TR-06531
itari@metu.edu.tr

Abstract

There are multiple and even interacting dimensions along which shape representation schemes may be compared and contrasted. In this paper, we focus on the following question. Are the building blocks in a compositional model localized in space (e.g. as in part based representations) or are they holistic simplifications (e.g. as in spectral representations)? Existing shape representation schemes prefer one or the other. We propose a new shape representation paradigm that encompasses both choices.

Introduction

Starting from 1960's, from the heavily numerical schemes to the structural ones, a variety of shape representation schemes have been proposed. Majority of them are compositional in the sense that the shape is constructed as an arrangement of building blocks which are in some sense *primitive*.

These building blocks provide a formation history of individual shapes; and they serve as primary search keys in comparing and contrasting shapes with each other. The primitive nature of building blocks are critical. They are either easier to manipulate than the whole shape; or they provide a clearer insight by amplifying relevant characteristics while attenuating irrelevant ones. Naturally, depending on the context which dictates what is relevant, there should be alternative ways for specifying the building blocks. Likewise, there are different ways of organizing the building blocks. At one extreme, the building blocks form an unordered collection. At the other extreme, the building blocks are organized as nodes of some graphical structure. It is appropriate to say that building blocks, together with the mechanism of organization form a representation scheme using which one can analyze and/or synthesize shapes.

There are multiple and even interacting dimensions along which shape representation schemes may be compared and contrasted. In this paper, we focus on the following question:

- Are the building blocks in a compositional model localized in space (e.g. as in part based representations) or are

they holistic simplifications (e.g. as in spectral representations)?

Existing shape representation schemes prefer one or the other. More often than not, the building blocks coincide with spatial parts (Biederman 1987)(Marr and Nishiara 1978)(Binford 1971)(Stiny and Gips 1972). It is however possible to define building blocks which are holistic simplifications over the entire shape domain as in Fourier representation where a given function is expressed as a linear combination of previously determined special functions (Reuter, Wolter, and Peinecke 2006)(Zuliani et al. 2004)(Maragos 1989).

We propose a new shape representation scheme that encompasses both choices.

Our scheme has two layers: the spectral and the spatial. The spectral layer is parameterized by a negative definite operator (defined on the shape domain) whose characteristic vectors serve as the elements of a dictionary. Along with their associated characteristic values, the characteristic vectors form an ordered set of holistic building blocks. The operator can be thought of as a mechanism of coding various local and global regularities.

The link between the spectral layer and the spatial layer is provided by a function which is used to introduce external bias. This function is the second parameter in our scheme, and in the absence of any external bias, it is selected as the indicator function of the shape domain. Thus, we refer to it as weighted or biased indicator function.

Passage to the spatial domain is achieved via spectral theorem. Note that any real valued function f defined on a given domain can be approximated as a linear combination of the characteristic vectors of a negative definite operator defined on that domain. Such an approximation is the closest function to f satisfying regularity constraints imposed by the operator. We view this approximate function as a field whose characteristics reveal part structure.

We emphasize that our representation which is parameterized by two parameters (i.e. a negative definite operator and a bias function) supports multiple interpretations of the same shape. In the next section we consider a variety of choices, each of which implying a different formation history and a different part structure. Such a capability is important because spatial parts are typically ambiguous when shapes are being analyzed in a purely bottom-up and context indepen-

dent manner without any reference to categorical units (Renninger 2003).

In a recent book, Stiny (2006) remarkably argues in favor of the continuous nature of shapes and ambiguity inherent in part perception. He demonstrates the possibility of infinitely many partitions (all interesting) and argues that it is this ambiguity that leads to creativity. Following Stiny (2006), Keles, Ozkar, and Tari (2010) present a computer implementation for part detection. Their methods relies on designer's preferences.

The work presented in this paper deals only with lower level biases.

The method

Let Ω represent a planar domain whose boundary is $\partial\Omega$. Let \mathcal{M} be a negative definite operator and let u and f be two functions, all defined on Ω . We consider the following equation:

$$\mathcal{M}u = f \quad (1)$$

subject to $u(x, y) = 0$ for $(x, y) \in \partial\Omega$.

Upon discretization, we obtain the following matrix equation:

$$\mathbf{M}\mathbf{u} = \mathbf{f} \quad (2)$$

where \mathbf{M} is an $N \times N$ the matrix representation of the discrete operator, and \mathbf{u} and \mathbf{f} are the vector representations of the sampled functions. Since \mathbf{M} is negative definite, it has a set of N orthonormal characteristic vectors with real characteristic values. Thus,

$$\mathbf{u} = \sum_{k=0}^N \frac{\langle \mathbf{v}_k, \mathbf{f} \rangle}{\lambda_k} \mathbf{v}_k \quad (3)$$

where λ_k, \mathbf{v}_k for $k = 1 \dots N$ are the characteristic value, characteristic vector pairs for the operator \mathbf{M} , and $\langle \cdot, \cdot \rangle$ denotes the inner product.

Observe the two representational layers. In the first layer, we have an expansion of \mathbf{u} as a series of functions which are the characteristic functions of \mathbf{M} . For example an obvious choice is the Laplace operator via which a local connectivity on a domain can be imposed (Tari 2010). The first six eigenvectors of the Laplace operator satisfying homogeneous Dirichlet conditions on the shape boundary (which is a square in this case) are depicted in Fig. 1.

In the second layer, we have a real valued function \mathbf{u} – the best approximation of \mathbf{f} in the spectrum of the operator \mathbf{M} . The function \mathbf{u} is a summary representation that combines the biased indicator function \mathbf{f} with the operator \mathbf{M} which codes assumed regularities within the shape domain.

On one hand, \mathbf{u} provides a partitioning of the shape into spatial parts. On one hand, the characteristic vectors form a set of holistic building blocks each of which spans the entire shape domain. They code the shape, prior to the bias introduced by \mathbf{f} . They are *primitive* or *atomic*, only with respect to the operator \mathbf{M} . The term $\frac{\langle \mathbf{v}_k, \mathbf{f} \rangle}{\lambda_k}$ given in (3) is the expression strength of the k^{th} characteristic vector. The expression strength is a function of the chosen shape indicator function \mathbf{f} and it suggests an alternative ordering of the characteristic vectors.

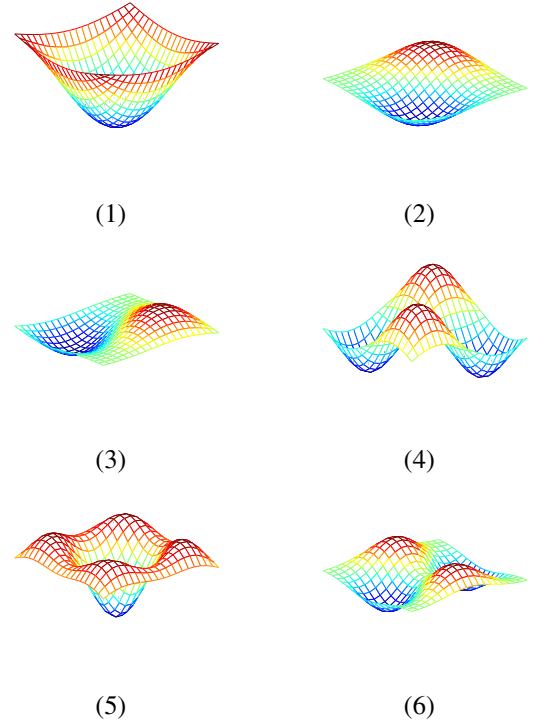


Figure 1: (1-6): The first six eigenvectors (for a square) of the Laplace operator with Dirichlet type boundary condition.

How to select \mathbf{M} and \mathbf{f}

There are former works in the literature which define a real valued function on the shape domain (which is later used for extracting shape knowledge) by solving a partial differential equation (PDE). In order to better situate our proposal, we relate it to these schemes.

The first scheme is by Tari, Shah, and Pien (1996; 1997) who propose the following PDE:

$$\begin{aligned} \Delta u - \alpha u &= -1 \\ u(x, y) &= 0 \text{ for } (x, y) \in \partial\Omega \end{aligned} \quad (4)$$

The solution $u(x, y)$ is the unique minimizer of an energy composed of two terms. The first term forces the function u be smooth. The second term forces the function u be equal to ones everywhere. These two constraints are conflicting if u is to satisfy homogenous Dirichlet condition on the shape boundary. The solution which is a trade-off between the two constraints is a smooth function which gradually increases to 1 as one moves away from the shape boundary towards the shape center (Tari, Shah, and Pien 1997; Tari 2009).

The discretization of the above PDE using Finite Difference Method yields (2) with $\mathbf{M} = \mathbf{L} - \alpha\mathbf{I}$ and $\mathbf{f} = -\mathbf{1}$ where \mathbf{L} is a matrix representation of the discrete Laplace operator and \mathbf{I} is the identity matrix.

The second PDE based scheme is presented by Gorelick et al. (2004; 2006). They propose to use the Poisson equation given below:

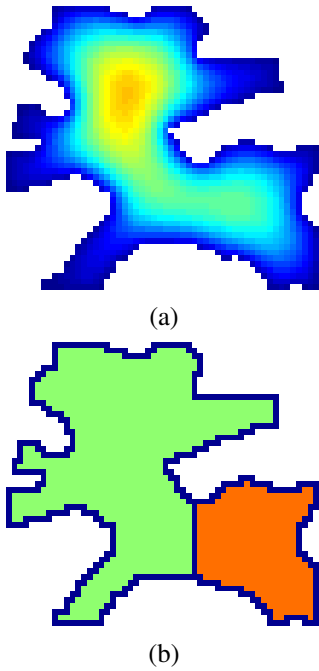


Figure 2: $M = L$ and $f = -1$ (a) u . (b) Two spatial parts implied by u are shown in different colors.

$$\begin{aligned} \Delta u &= -1 \\ u(x, y) &= 0 \text{ for } (x, y) \in \partial\Omega \end{aligned} \quad (5)$$

Notice that (5) is a special case of (4) with $\alpha = 0$.

The discretization of (5) coincides with (2) when $M = L$ and $f = -1$.

In the first experiment depicted Fig. 2, these settings are used. The result is illustrated using a sample shape drawn on a 50×55 lattice and composed of 1640 pixels. Fig. 2 (a) depicts u . Notice that u has two local maxima indicating two spatial parts. One can consider a growth starting from each local maxima till one reaches a saddle point, to extract the scope of each part. In Fig. 2 (b), the implied partitioning is depicted.

In the second experiment depicted in Fig. 3, we discuss the influence of f by setting it equal to the distance transform of a circle as shown in Fig. 3 (a). The function u is depicted in Fig. 3 (b)-(c). Notice that there is only one local maxima. In this case, no further partitioning is implied and the entire shape is interpreted as a single piece.

In the third experiment depicted in Fig. 4 we obtained a new operator by changing the ordering of the characteristic values of L . Specifically, we set the first characteristic value to a value which is smaller than the last characteristic value. (The first and the last characteristic values of L are -0.0263 and -7.9737 , respectively. We have set the first one to -8 , the largest integer which is smaller than -7.9737 .) The effect of this modification is to suppress the first characteristic function which is positive everywhere. The second characteristic function dominates the result. u attains both neg-

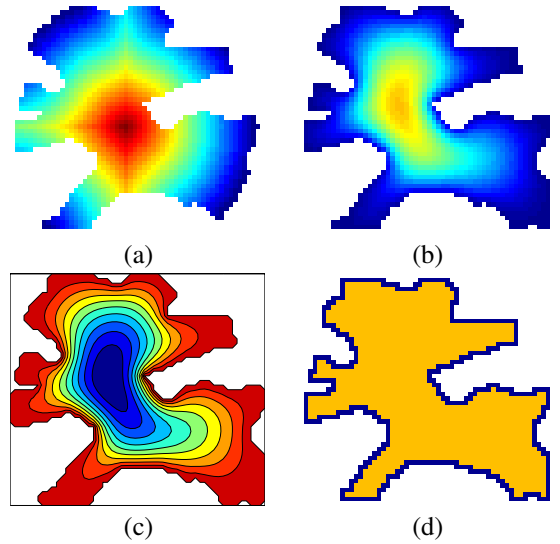


Figure 3: A biased indicator function: f is the distance transform of a circle. (a) f . (b) u . (c) contour plot of u . (d) The shape is interpreted as a single piece.

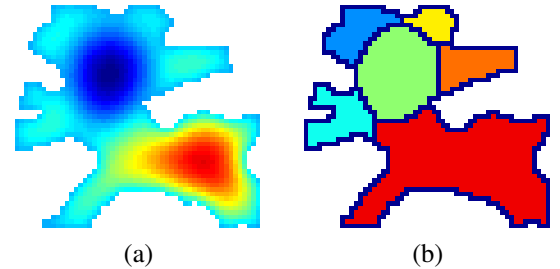


Figure 4: A new operator M is obtained from L by changing the ordering of the characteristic values of L . (a) u . (b) Seven spatial parts implied by u are shown in different colors.

ative and positive values. The respective contour plots are depicted in Fig. 5.

We remark that one can no longer relate the new scheme given in (2) to a PDE when the operator M is constructed this way.

In the fourth experiment which is similar to the third experiment, we obtained a new operator by setting both the first and the second characteristic values to -8 . The effect of this modification is to suppress the first two characteristic functions. The third characteristic function dominates in the result. The result is depicted in Fig. 6. The part structure has a different character than the previous part structures. There is a central blob which looks like a coarser form of the initial shape. This blob is separated from the peripheral part by a sign change in u (Fig. 6-(a)). The peripheral structure is attached to this coarse central structure. (The respective contour plots are depicted in Fig. 7.)

In the final experiment we set $M = L - J$ where J is the matrix of ones; and set f to the distance transform

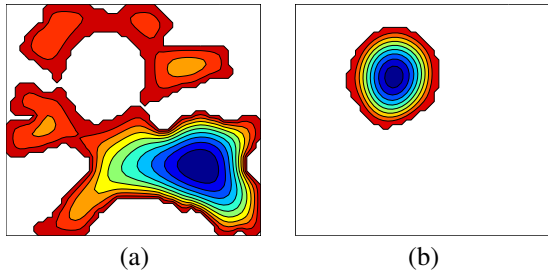


Figure 5: Contour plots of u . (a) where it is positive. (b) where it is negative.

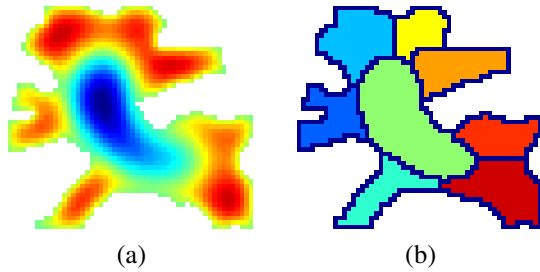


Figure 6: A new operator M is obtained from L by changing the ordering of the characteristic values of L . (a) u . (b) Eight spatial parts implied by u are shown in different colors.

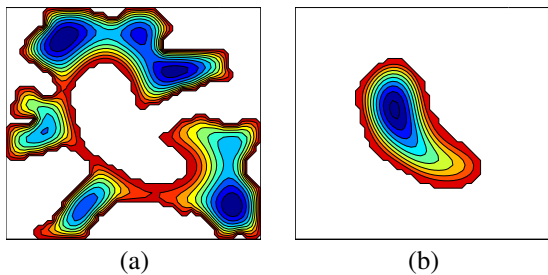


Figure 7: Contour plots of u . (a) where it is positive. (b) where it is negative.

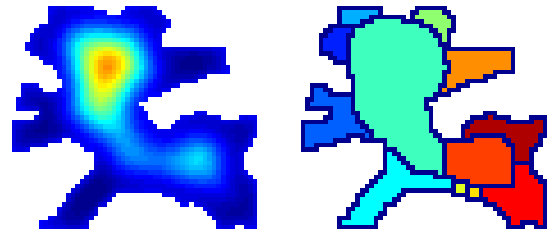


Figure 8: $M = L - J$ where J is the matrix of ones (Tari 2009). (a) u . (b) Spatial parts implied by u are shown in different colors.

of the shape. (Such a model is equivalent to a recent modification of the method of Tari, Shah, and Pien (1996; 1997) by Tari (2009).) M has two terms. The first term L forces a local regularity inside the shape domain as in PDE based schemes. However, the second term J forces a global regularity over the entire shape domain. The new model can no longer be expressed as a PDE. The perceptual implications are discussed in (Tari 2010).

Result of the final experiment is depicted in Fig. 8. Notice the resemblance of the implied part structure to the one in Fig. 6. There is a central blob, again, which is separated from the peripheral part by a sign change in u (6-(a)). This time the central structure is composed of two parts shown in different shades of gray. This type of partitioning can be related to a remark that global shape is separate from the peripheral detail (Koenderink and van Doorn 1982)(Navon 1977).

A noisy shape (*prickly pear*) shown in Fig. 9 (a) further demonstrates the implication of such a separation. Majority of the partitioning schemes will decompose the prickly pear into two blobs as shown in Fig. 9 (b). This result is taken from (Zeng et al. 2008). The partitioning is computed by using both boundary concavities and local symmetry axes. In our new scheme if $M = L$, similar partitioning is obtained. However, when $M = L - \alpha J$, the part structure changes.

As shown in Fig. 10, the shape is split into a peripheral structure (light gray) and a coarse global shape (shown as the union of two darker shades). This suggests a different formation history than the partitioning given in Fig. 9 (b). Whereas the former one (Fig. 9 (b)) implies that two prickly balls are glued together, the latter one (Fig. 10) implies that two smooth balls are glued together and a boundary detail or noise is added later.

The partitioning into peripheral structure and coarse structure is also implied when the operator of the fourth experiment is used (Fig. 11).

Summary and Discussion

We presented a new shape representation paradigm which is compositional yet support multiple interpretations. The building blocks are expressible either in the form of spatial parts organized graphically, or in the form of characteristic functions ordered with respect to their expression strength.

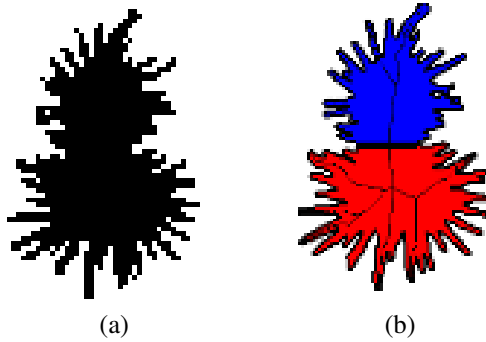


Figure 9: A noisy shape composed of two blobs. See text.

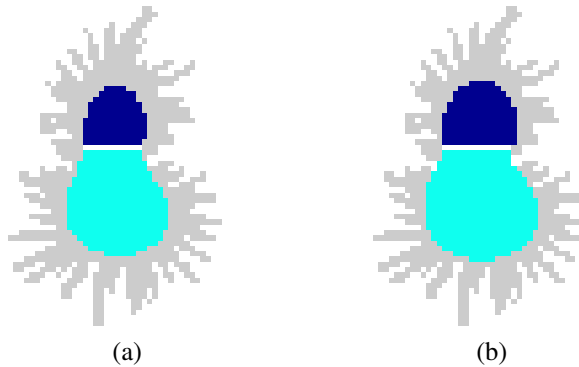


Figure 10: The partitioning when $M = L - \alpha J$. (a) $\alpha = 1$. (b) $\alpha = 0.5$.

Shape primitives vary with the choice of an operator coding the regularities within the shape domain and a biased indicator function.

The new representation supports multiple perspectives on the formation history of the shape. Supporting multiple interpretations at the computational level is important. Parts are ambiguous (when considered without reference to categorical units (Renninger 2003)) and as Stiny (2006) remarkably argues they should be.

Acknowledgements

The work is partially funded by TUBITAK under grant 108E015.

References

- Biederman, I. 1987. Recognition-by-components: A theory of human image understanding. *Psychological Review* 94(2):115–117.
- Binford, T. 1971. Visual perception by computer. In *IEEE Conference on Systems and Control*.
- Gorelick, L.; Galun, M.; Sharon, E.; Basri, R.; and Brandt, A. 2004. Shape representation and classification using the poisson equation. In *CVPR (2)*, 61–67.
- Gorelick, L.; Galun, M.; Sharon, E.; Basri, R.; and Brandt, A. 2006. Shape representation and classification using the

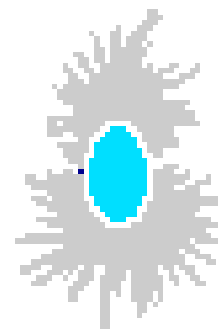


Figure 11: The partitioning when M is chosen as the operator from the fourth experiment.

poisson equation. *IEEE Trans. Pattern Anal. Mach. Intell.* 28(12):1991–2005.

Keles, H.; Ozkar, M.; and Tari, S. 2010. Embedding shape without predefined parts. *Environment and Planning B*.

Koenderink, J. J., and van Doorn, A. J. 1982. The shape of smooth objects and the way contours end. *Perception* 11:129–137.

Maragos, P. 1989. Pattern spectrum and multiscale shape representation. *IEEE Trans. Pattern Anal. Mach. Intell.* 11(7):701–716.

Marr, D., and Nishiara, H. K. 1978. Representation and recognition of spatial organization of three dimensional shapes. In *Proceedings of the Royal Society of London, Series B, Biological Sciences*, 200, 269–294.

Navon, D. 1977. Forest before trees: The precedence of global features in visual perception. *Cognitive Psychology* 9:355–383.

Renninger, L. W. 2003. *Parts, Objects and Scenes: Psychophysics and Computational Models*. Ph.D. Dissertation, UC Berkeley, USA.

Reuter, M.; Wolter, F.; and Peinecke, N. 2006. Laplace-beltrami spectra as shape-dna of surfaces and solids. *Computer-Aided Design* 38(4):342–366.

Stiny, G., and Gips, J. 1972. Shape grammars and the generative specification of painting and sculpture. In Petrocelli, P., ed., *The Best Computer Papers of 1971*. Auerbach, Philadelphia. 125–135.

Stiny, G. 2006. *Shape: Talking about Seeing and Doing*. MIT Press.

Tari, S.; Shah, J.; and Pien, H. 1996. A computationally efficient shape analysis via level sets. In *MMBIA '96: Proceedings of the 1996 Workshop on Mathematical Methods in Biomedical Image Analysis (MMBIA '96)*, 234–243.

Tari, S.; Shah, J.; and Pien, H. 1997. Extraction of shape skeletons from grayscale images. *CVIU* 66(2):133–146.

Tari, S. 2009. Hierarchical shape decomposition via level sets. In *International Symposium on Mathematical Morphology*, 217–228.

Tari, S. 2010. Extracting parts of 2d shapes using local and global interactions simultaneously. In Chen, C., ed., *Hand-*

book of Pattern Recognition and Computer Vision. World Scientific.

Zeng, J. T.; Lakaemper, R.; Wei, X.; and Li., X. 2008. 2d shape decomposition based on combined skeleton-boundary features. In *Advances in Visual Computing, 4th International Symposium, ISVC*, 682–691.

Zuliani, M.; Kenney, C.; Bhagavathy, S.; and Manjunath, B. S. 2004. Drums and curve descriptors. *UCSB Vision Research Lab Preprint*.